Cancer Cell
Article

CCL18 from Tumor-Associated Macrophages Promotes Breast Cancer Metastasis via PITPNM3

Jingqi Chen,[1,2,5] Yandan Yao,[1,5] Chang Gong,[1,5] Fengyan Yu,[1,5] Shicheng Su,[1] Jianing Chen,[1] Bodu Liu,[1] Hui Deng,[3] Fengsong Wang,[3] Ling Lin,[1] Herui Yao,[1] Fengxi Su,[1] Karen S. Anderson,[4] Qiang Liu,[1,4] Mark E. Ewen,[4] Xuebiao Yao,[3,*] and Erwei Song[1,*]

[1]Breast Tumor Center, Sun-Yat-Sen Memorial Hospital, Sun-Yat-Sen University, Guangzhou 510120, China
[2]Department of Medical Oncology, No. 2 Affiliated Hospital, Guangzhou Medical College, Guangzhou 510260, China
[3]Anhui Key Laboratory for Cellular Dynamics & Chemical Biology, Hefei National Laboratory for Physical Sciences at Nanoscale, and University of Science & Technology of China, Hefei, Anhui 230027, China
[4]Department of Medical Oncology, Dana-Farber Cancer Institute, Harvard Medical School, Boston, MA 02115, USA
[5]These authors contributed equally to this work
*Correspondence: songerwei02@yahoo.com.cn (E.S.), yaoxb@ustc.edu.cn (X.Y.)
DOI 10.1016/j.ccr.2011.02.006

SUMMARY

Tumor-associated macrophages (TAMs) can influence cancer progression and metastasis, but the mechanism remains unclear. Here, we show that breast TAMs abundantly produce CCL18, and its expression in blood or cancer stroma is associated with metastasis and reduced patient survival. CCL18 released by breast TAMs promotes the invasiveness of cancer cells by triggering integrin clustering and enhancing their adherence to extracellular matrix. Furthermore, we identify PITPNM3 as a functional receptor for CCL18 that mediates CCL18 effect and activates intracellular calcium signaling. CCL18 promotes the invasion and metastasis of breast cancer xenografts, whereas suppressing PITPNM3 abrogates these effects. These findings indicate that CCL18 derived from TAMs plays a critical role in promoting breast cancer metastasis via its receptor, PITPNM3.

INTRODUCTION

The tumor microenvironment comprises a variety of nonmalignant stromal cells that play a pivotal role in tumor progression and metastasis (Robinson et al., 2009). Among them, tumor-associated macrophages (TAMs) are the most notable migratory hematopoietic cell type (Mantovani and Sica, 2010; Solinas et al., 2009). Evidence from clinical and epidemiological studies has shown a strong association between TAM density and poor prognosis in several types of cancer (Condeelis and Pollard, 2006; Pollard, 2004), including breast cancer (Mantovani et al., 2007).

Macrophages are heterogeneous cells that respond differently to various microenvironmental signals and, thus, display distinct functions (Gordon, 2003; Martinez et al., 2009). Breast TAMs are primarily a macrophage subpopulation with M2 phenotype activated by interleukin-4 (IL-4) produced by $CD4^+$ T cells (DeNardo et al., 2009). Further mechanistic studies reveal that TAMs promote breast cancer progression and metastasis by releasing a variety of cytokines, including chemokines, inflammatory factors, and growth factors (Condeelis and Pollard, 2006; Gocheva et al., 2010). TAM-derived cytokines may promote the invasiveness of tumor cells by enhancing their adhesion to extracellular matrix (ECM) in the tumor stroma (Pittet, 2009). Previous studies have identified several factors important for TAM-promoted tumor progression, including EGF, VEGF, and MMP7/9 (Coussens et al., 2000; Dirkx et al., 2006; Goswami et al., 2005; Leek et al., 2002). However, these factors are also produced by cancer cells themselves, and such autocrine signaling also contributes to cancer development (Lichtenberger et al., 2010). Currently, the cytokine profile of TAMs remains largely unknown, and it is unclear whether there are some exclusively TAM-derived cytokines that are functionally essential to tumor progression.

Significance

The infiltration level of tumor-associated macrophages (TAMs) is associated with poor prognosis in patients with breast cancer, but the underlying mechanisms were not clear. Through the analysis of cytokine profile of breast TAMs, we find that CCL18 is abundantly expressed, and the CCL18 level in blood or cancer stroma is associated with metastasis of patients with breast cancer. CCL18 is critical for breast TAMs to promote the migration and invasion of breast cancer cells. We identify PITPNM3 as a functional receptor for CCL18 in promoting metastasis. Our study shows that CCL18 is an important TAM-derived cytokine in promoting breast cancer metastasis and suggests that CCL18-PITPNM3 interaction is crucial to the activation of intracellular calcium signaling and enhanced invasiveness of breast cancer cells.

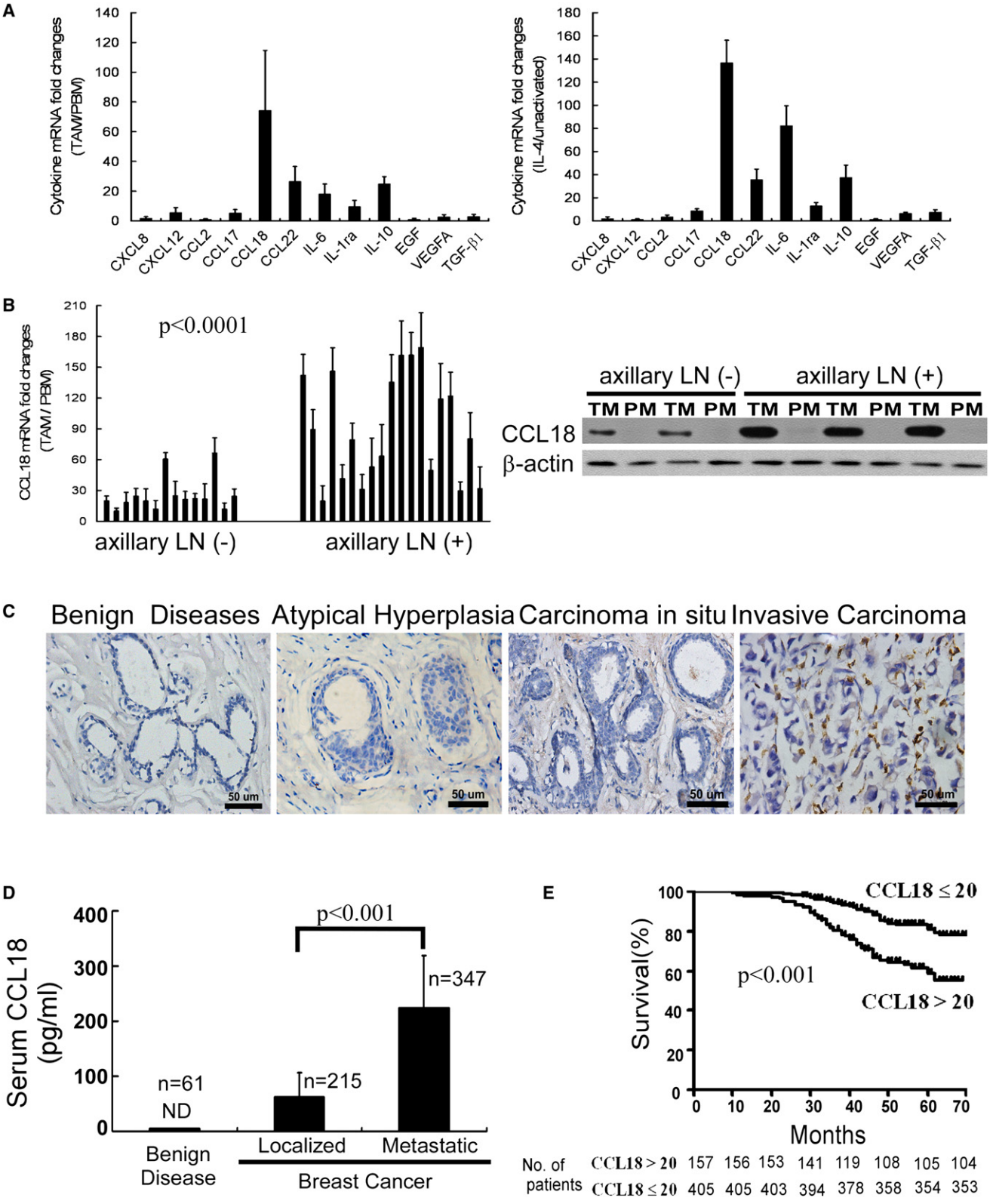

Figure 1. Breast TAMs Constitutively Express CCL18

(A) The ratio of a panel of cytokine mRNA in TAMs versus PBMs from patients with breast cancer and IL-4-activated MDMs versus unactivated MDMs from healthy donors, as assayed by qRT-PCR.

Chemokine (C-C motif) ligand 18 (CCL18) is a chemokine predominantly produced by monocyte-derived cells with M2 phenotype (Kodelja et al., 1998). Excessive production of CCL18 in M2 macrophages was demonstrated in various chronic inflammations and fibrotic diseases, including Gaucher's disease and rheumatoid arthritis (Martinez et al., 2009; Schutyser et al., 2005). In addition, constitutive expression of CCL18 was observed in macrophages infiltrating ovarian cancer, gastric cancer, and glioma (Chang et al., 2010; Leung et al., 2004; Schutyser et al., 2002; Zohny and Fayed, 2010). However, the role of CCL18 in cancer progression is controversial. CCL18 was reported to participate in immunosuppression of ovarian cancer (Duluc et al., 2009; Zohny and Fayed, 2010) but was associated with prolonged survival in patients with gastric cancer (Leung et al., 2004). Although M2 macrophages are abundant in breast cancer stroma, the role of CCL18 in breast tumor progression remains elusive. Furthermore, understanding of CCL18 function is hampered by the fact that CCL18 receptor and the underlying pathways remain unknown. In this study we aimed to investigate the contribution of CCL18 in breast cancer metastasis and to identify the receptor and signaling pathway that mediate CCL18 effects.

RESULTS

CCL18 Expression in Breast TAMs Correlates with Tumor Invasiveness

Because breast TAMs are primarily M2 macrophages activated by Th2 cytokines, most notably IL-4 (DeNardo et al., 2009), we performed quantitative RT-PCR (qRT-PCR) to screen a panel of cytokines related to M2 macrophages (Gordon, 2003) in paired TAM and peripheral blood monocyte (PBM) samples isolated from six patients with invasive ductal breast carcinomas, and in IL-4-treated versus untreated monocyte-derived macrophages (MDMs) obtained from six healthy donors. The mRNA profile of M2-related cytokines in TAMs was analogous to that in IL-4-activated MDMs. Among all the cytokines tested, CCL18 is the most abundantly expressed cytokine in both TAMs and IL-4-activated M2 cells (Figure 1A).

To confirm CCL18 expression in breast TAMs, we examined the mRNA and protein expression of the chemokine in paired TAM and PBM samples isolated from another set of 33 patients with invasive breast carcinomas. Examined by qRT-PCR, CCL18 mRNA was 25 ± 17-fold higher in TAMs than PBMs in 14 patients with breast cancer without regional lymph node metastasis, whereas it was 91 ± 52-fold higher in the other 19 patients with axillary lymph node metastasis (Figure 1B; $p < 0.0001$). Western blotting also showed that CCL18 protein was only identified in TAMs, but not in PBMs, of patients with breast cancer, and its expression was much stronger in the patients with axillary lymph node metastasis than those without metastasis (Figure 1B). Likewise, CCL18 mRNA and protein were dramatically upregulated in IL-4-activated M2 cells, whereas only slightly elevated in LPS-activated M1 cells, but were not detected in unactivated MDMs, or MDA-MB-231 cells, a breast cancer line with metastasis potential, or MCF-10A, an immortalized breast epithelial line (see Figures S1A and S1B available online). Furthermore, IL-4-activated M2 cells produced abundant amount of CCL18 protein in their supernatants determined by ELISA (Figure S1E). The specificity of CCL18 expression and production in IL-4-activated M2 cells was confirmed by transfecting the cells with small interfering RNAs (siRNAs) targeting CCL18 mRNA (Figures S1C and S1D).

Immunohistochemistry for CCL18 expression in breast cancer tissues revealed that CCL18-positive cells were observed scattered in the tumor stroma of 505 out of 562 cases of invasive breast carcinomas (Figure 1C). However, no staining was observed in the neoplastic cells and the adjacent non-neoplastic epithelia. Additionally, $CCL18^+$ cells were absent in all benign breast tissues, including fibrocystic lesions with or without atypical epithelial hyperplasia, whereas they were occasionally identified in the stroma of 11 out of 57 cases of ductal carcinomas in situ (DCIS) of the breast (Figure 1C). Furthermore, confocal microscopy revealed colocalization of CCL18 and CD68 immunostaining, a marker for macrophages, in breast cancer tissues, confirming that CCL18 immunostaining cells were subsets of macrophages (Figure S1F).

We next correlated $CCL18^+$ TAM counts with the clinicopathological status of patients with breast cancer (Table 1). The number of $CCL18^+$ TAMs increased with higher tumor burden defined by tumor size ($p = 0.044$) and staging ($p < 0.001$), and aggressive tumor biology by advanced histopathological grading ($p = 0.002$) and lymphovascular invasion (LVI; $p < 0.001$). However, there was no observed difference in $CCL18^+$ TAM counts according to estrogen receptor (ER) status ($p = 0.31$). Yet, $CCL18^+$ TAMs increased with $CD4^+$ lymphocytic infiltration in cancer stromas ($p = 0.036$; Figure S1G). Additionally, $CCL18^+$ TAMs were more abundant in the primary tumors with axillary lymph node ($p < 0.01$) and distal metastasis ($p = 0.014$) but was unrelated to the proliferation of cancer cells, determined by Ki67 and PCNA expression ($p > 0.05$; Table S2). CCL18 protein level in the serum of patients with breast cancer with lymph node or distal metastasis was also significantly higher than those without metastasis (Figure 1D; $p < 0.001$). Consistent results were obtained when a different cutoff of $CCL18^+$ TAM counts was applied (Table S1). These data imply that CCL18 produced by TAMs correlates with the invasiveness but not the growth kinetics of breast tumor cells. However, $CCL18^+$ macrophage counts in the primary breast tumors were much higher

(B) The ratio of CCL18 mRNA in TAMs versus PBMs from patients with breast cancer (n = 33) with or without axillary lymph node metastasis, as determined by qRT-PCR (left). Each bar corresponds to mean ± standard deviation (SD) of each individual patient. Representative western blotting for CCL18 in TAMs and PBMs from patients with breast cancer with or without axillary lymph node metastasis (right). β-Actin was used as a loading control.
(C) Immunohistochemical staining of CCL18 in benign cystic fibrosis of the breast, atypical hyperplasia, breast carcinoma in situ, and invasive breast carcinoma.
(D) Serum CCL18 level in the patients with benign breast diseases and invasive breast carcinomas with or without axillary lymph node or distal metastasis, as determined by ELISA. Bars correspond to mean ± SD.
(E) Kaplan-Meier survival curve of patients with breast cancer with lower (≤20 per view of field, n = 405) and higher CCL18-positive TAM counts (>20 per view of field, n = 157; $p < 0.001$) with a median follow-up period of 45 months. The number of survived patients stratified to the follow-up periods is indicated below the graph.
See also Figure S1.

Table 1. Correlation of CCL18 Expressing TAM Counts with Clinicopathological Status in 562 Cases of Patients with Breast Cancer

$CCL18^+$ TAM Counts	≤5	6–20	>20	p Value
Age (years)				
≤45	126	75	69	
>45	106	99	87	0.716
Tumor Size (cm)				
≤2	126	75	69	
>2	106	98	88	0.044
Stage				
0	46	10	1	
I	73	13	1	
II	107	97	92	
III	6	53	63	<0.001
Histological Grade[a]				
I	45	46	17	
II	72	60	64	
III	69	57	75	0.002
Metastasis[b]				
Lung	2	4	7	
Liver	0	13	12	
Bone	4	25	27	
Brain	1	3	7	0.014
Lymph Node Metastasis				
0	165	33	17	
1–3	58	84	70	
≥4	9	56	70	<0.01
LVI				
(+)	32	61	91	
(–)	200	112	66	<0.001
ER				
(+)	162	129	120	
(–)	70	44	37	0.31
Her2				
(+)	34	25	41	
(–)	197	147	117	0.007
CCL5				
(–)	59	44	45	
(+)	61	53	39	
(++)	68	47	35	
(+++)	44	28	39	0.364
CD4+ T Lymphocytes[c]				
Low	90	58	46	
Media	88	57	53	
High	54	58	58	0.036
CD8+ T Lymphocytes[c]				
Low	85	49	55	
Media	74	66	58	
High	73	57	45	0.414

See also Tables S1–S3.
[a] Grading in 505 cases of invasive ductal carcinoma.
[b] Distant metastasis identified during postoperative follow-up.
[c] Percent volume of $CD4^+/CD8^+$ T lymphocytes.

than their corresponding metastatic lesions in the lymph node, liver, lung, and brain (Figure S1H), suggesting that CCL18 produced by TAMs probably affects the primary tumors in a paracrine manner.

Kaplan-Meier survival curve with a median follow-up period of 45 months demonstrated that patients with low $CCL18^+$ TAM count (≤20), as defined elsewhere (Leung et al., 2004), survive significantly longer than those with high $CCL18^+$ cell counts (>20) (Figure 1E; $p < 0.001$). In a multivariate Cox regression analysis, $CCL18^+$ TAM count was associated with poor survival prognosis of patients with breast cancer (hazard ratio, 1.47; $p = 0.022$), independent of other clinical covariates (Table S3), indicating that CCL18 is an independent prognostic factor for breast cancer. However, our cohort did not show any significant correlation of patient prognosis with ER expression or LVI.

TAMs and IL-4-Activated MDMs Promote the Invasiveness of Breast Cancer Cells via CCL18

Boyden chambers were used to examine the invasiveness of breast cancer cells by plating them on fibronectin-coated inserts with macrophages in the lower wells. Compared with MDA-MB-231 cells in medium alone, the number of invading cancer cells upon coculturing for 8 hr with resting or LPS-activated MDMs increased by 66% ($p < 0.05$) and 2-fold ($p < 0.01$), respectively, and more dramatically by nearly 11-fold with IL-4-activated MDMs ($p < 0.001$; Figure 2A). The direct influence of LPS and IL-4 on the invasiveness of cancer cells was ruled out by adding these mediators alone in the lower chambers (data not shown). Similarly, the invasiveness of MDA-MB-231 cells and primary breast cancer cells was enhanced by 6- and 9-fold, respectively, upon coculturing with TAMs isolated from primary breast tumor samples, whereas only by 2- and 3-fold, respectively, with the macrophages derived from PBMs of the same patients (Figure 2B). Thus, mediators released by TAMs or IL-4-activated MDMs promote the invasiveness of breast cancer cells in vitro.

To determine whether CCL18 contributes to cancer cell invasion, we employed a polyclonal anti-CCL18 antibody that was shown by R&D Systems to neutralize CCL18 function in lymphocytes, as well as the two CCL18-siRNAs. In the presence of LPS- or IL-4-activated macrophages, the number of invasive cancer cells was reduced by 27% and 53%, respectively, by adding anti-CCL18 antibody at 5 μg/ml, and by 40% and 73%, respectively, at 10 μg/ml, but not by an isotype-matched IgG at 10 μg/ml (Figure 2A). However, anti-CCL18 antibody itself did not influence the invasion of cancer cells in culture medium alone or cocultured with unactivated macrophages that do not express CCL18 (Figure 2A). Addition of anti-CCL18 antibody to the coculture system of primary TAMs with MDA-MB-231 line or primary breast cancer cells also reduced the number of invasive cancer cells in a dose-dependent manner (Figure 2B; $p < 0.01$). Transfection of IL-4-activated MDMs with either of the two CCL18-siRNAs also reduced the number of invasive cancer cells by 75% and 70%, respectively (Figure 2C). Furthermore, treatment of MDA-MB-231 and SKBR3 line with recombinant CCL18 (rCCL18, 0–20 ng/ml) for 8 hr enhanced the invasion of cancer cells in a dose-dependent manner, whereas treatment of 20 ng/ml rCCL20, a member from the same chemokine family, had no effect (Figure 2D; Figure S2D). However, incubation of MDA-MB-231 cells with rCCL18 at 20 ng/ml for up to 24 hr did

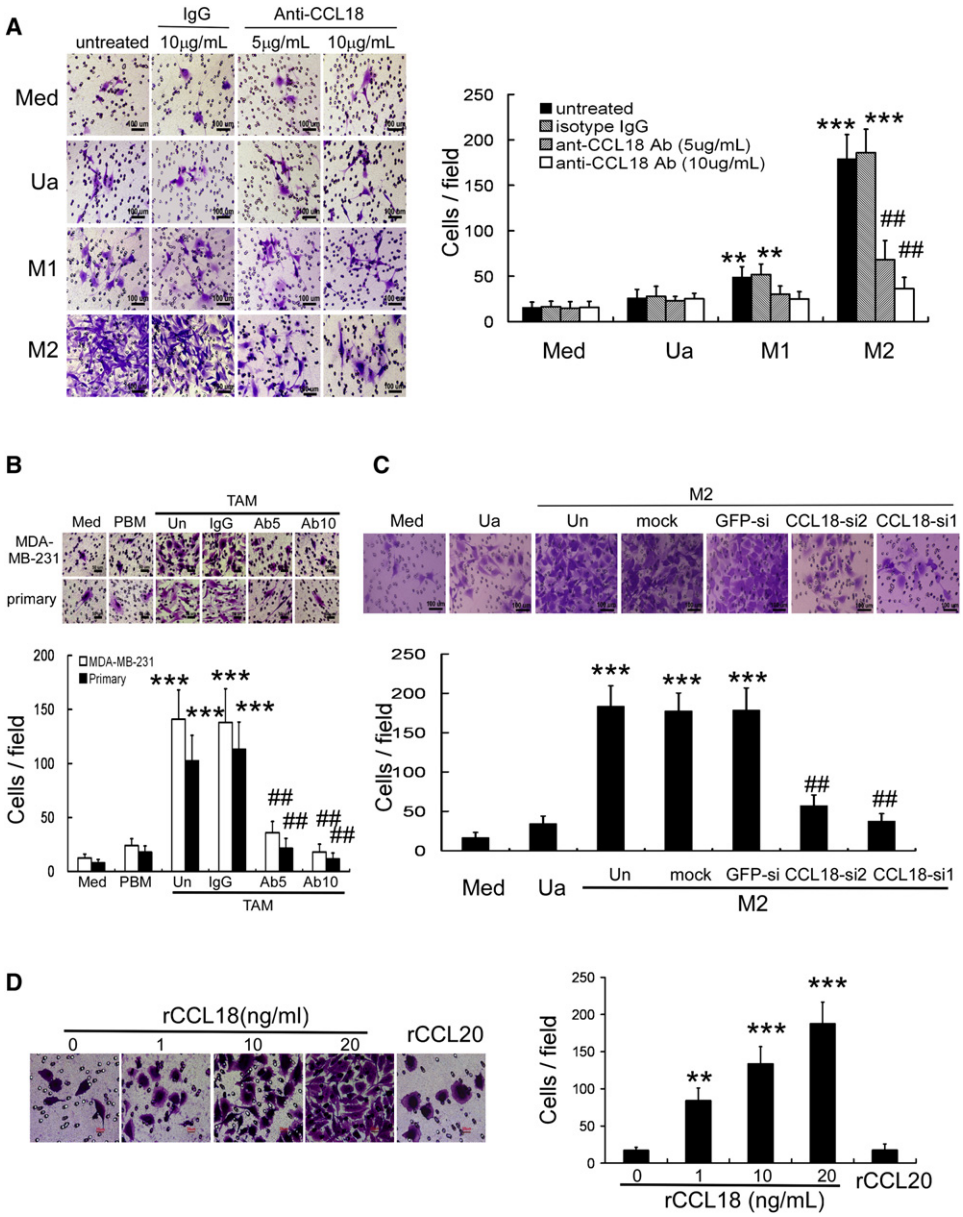

Figure 2. Breast TAMs and IL-4-Activated MDMs Promote the Invasion of Breast Cancer Cells via CCL18

(A) Boyden chamber assay for MDA-MB-231 cells plated on the upper cell culture inserts, with culture medium alone (Med), unactivated (Ua), LPS-activated (M1), or IL-4-activated MDMs (M2) plated in the lower chambers in the presence or absence of an anti-CCL18 antibody at 5 or 10 μg/ml, or an isotype-matched IgG control (IgG).

(B) Similar to (A), MDA-MB-231 cells or primary breast cancer cells were cocultured with PBMs or TAMs from patients with breast cancer plated.

(C) Similar to (A), MDA-MB-231 cells were cocultured with unactivated (Ua) MDMs or IL-4-activated MDMs (M2) that were untreated (Un), mock transfected, or transfected with either of the two CCL18-siRNAs or GFP-siRNA.

(D) Boyden chamber assay for MDA-MB-231 cells with rCCL18 at increasing concentrations (1–20 ng/ml) or rCCL20 at 20 ng/ml added to culture medium in the lower chambers. Bars correspond to mean ± SD. **p < 0.01 and ***p < 0.001 as compared with the cells treated with medium alone, whereas ## p < 0.01 as compared with the untreated cells cocultured with M2 MDMs or TAMs.

See also Figure S2.

not influence cancer cell proliferation, determined by BrdU staining, soft agar assay, and [^{3}H]incorporation assay (Figures S2A–S2C). Collectively, these data suggest that both IL-4-activated macrophages and TAMs promote the invasiveness of breast cancer cells via CCL18.

CCL18 Enhances ECM Adherence and Migration of Breast Cancer Cells

To explore the mechanism that CCL18 promotes invasion, we investigated whether CCL18$^+$ macrophages induce the adherence of breast cancer cells to fibronectin, the most

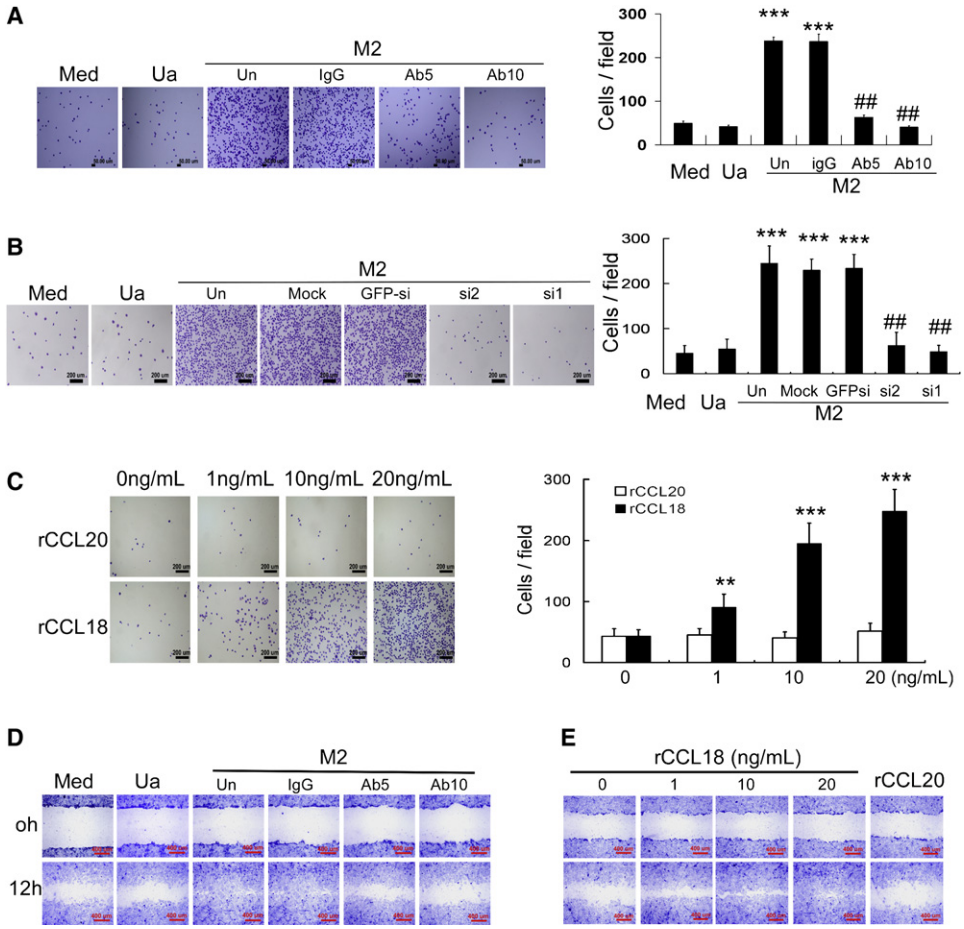

Figure 3. IL-4-Activated MDMs Promote Fibronectin Adherence and Migration of Breast Cancer Cells via CCL18

(A) Adherence assays for MDA-MB-231 cells suspended in serum-free medium in the lower wells of the Boyden chambers coated with fibronectin, with or without (Med) unactivated (Ua) or IL-4-activated MDMs (M2) plated on the inserts in the presence or absence of an anti-CCL18 antibody at 5 μg/ml (Ab5) or 10 μg/ml (Ab10), or an isotype-matched IgG control (IgG).

(B) Similar to (A), MDA-MB-231 cells were cocultured with unactivated (Ua) or IL-4-activated MDMs (M2) that were untransfected (Un), mock transfected, or transfected with either of the two CCL18-siRNAs (si1 and si2) or GFP-siRNA.

(C) MDA-MB-231 cells were suspended in serum-free medium and allowed to adhere to culture plate coated with fibronectin in the presence or absence of rCCL18 and rCCL20 at increasing concentrations (1–20 ng/ml). Bars correspond to mean ± SD. $^{**}p < 0.01$ and $^{***}p < 0.001$ as compared with the cells treated with medium alone, whereas ## $p < 0.01$ as compared with the untreated cells cocultured with M2 MDMs.

(D) Wound-healing assay for MDA-MB-231 cells plated in the lower Boyden chambers, with unactivated (Ua) or IL-4-activated MDMs (M2) seeded on cell culture inserts in the presence or absence (Un) of an anti-CCL18 antibody at 5 μg/ml (Ab5) or 10 μg/ml (Ab10), or an isotype-matched IgG control (IgG).

(E) Wound-healing assay for MDA-MB-231 cells in the presence or absence of rCCL18 at increasing concentration (1–20 ng/ml) or rCCL20 at 20 ng/ml.

See also Figure S3.

abundant ECM component in the stroma of breast cancer (Simpson-Haidaris and Rybarczyk, 2001). In a Boyden chamber where macrophages were plated on the 0.4 μm cell culture inserts, cancer cells were suspended in serum-free media in the lower wells coated with fibronectin. After 60 min of coculture, IL-4-activated MDMs dramatically increased the number of cancer cells adherent to fibronectin as compared with unactivated MDMs or culture medium alone, which was blocked by the anti-CCL18 antibody in a dose-dependent manner (Figure 3A; $p < 0.01$). Consistent with the finding above, IL-4-activated MDMs transfected with CCL18-siRNA significantly lost their ability to promote the adherence of cancer cells to fibronectin (Figure 3B; $p < 0.01$). Moreover, treatment of suspended MDA-MB-231 cells with rCCL18 for 60 min enhanced their adherence to fibronectin in a dose-dependent manner (Figure 3C).

Wound-healing assay was used to evaluate the effect of $CCL18^{+}$ macrophages on cancer cell migration, another hallmark contributing to the invasion and metastasis of cancers. MDA-MB-231 cells were plated in the lower wells of Boyden chamber and cocultured for 12 hr with macrophages that were seeded on 0.4 μm inserts, allowing only cytokine but not cellular communication between the upper and lower chambers. Cancer cells that were exposed to IL-4-activated MDMs migrated more rapidly to close the scratched wounds compared with those exposed to resting MDMs or culture media alone. Addition of anti-CCL18 antibody inhibited the effect of IL-4-activated MDMs on cancer cell migration in a dose-dependent manner

(Figure 3D; Figure S3A). Moreover, incubation of MDA-MB-231 or SKBR3 cells with rCCL18 (0–20 ng/ml) dose dependently promoted the migration of cancer cells (Figure 3E; Figure S3B). These results indicate that CCL18 is critical for TAMs to promote ECM adherence and migration of breast cancer cells.

PITPNM3 Is a Transmembrane Receptor for CCL18 Activities

To evaluate whether a potential receptor for CCL18 exists at the breast cancer cell membrane, MDA-MB-231 cells were incubated with rCCL18 for 3 hr at 4°C, fixed, and then stained with an Alexa 488-labeled anti-CCL18 antibody. Immunofluorescence showed that CCL18 was localized to cell membrane (Figure 4A), implying that specific molecules on the cancer cell surface may mediate the biological effects of CCL18. Addition of the anti-CCL18 antibody during incubation prevented CCL18 localization to cell membrane (Figure S4A), validating its neutralizing function in breast cancer cells.

To identify the unknown receptor of CCL18 function, the membranous proteins of rCCL18-treated MDA-MB-231 cells were extracted, immunoprecipitated with a monoclonal anti-CCL18 antibody that has no neutralizing function, and resolved on a denaturing gel. A specific protein band was revealed by Coomassie blue staining in the resultant immunoprecipitate (lane 7, Figure 4B) and analyzed by liquid chromatography-mass spectrometry. The protein band was identified to be a membrane-associated phosphatidylinositol transfer protein 3, PITPNM3 (also named PYK2 N-terminal domain-interacting receptor 1, Nir1), a human homolog of the *Drosophila* retinal degeneration B (*rdgB*) (Figure 4C). This was further confirmed by immunoblotting of the immunoprecipitate with an anti-PITPNM3 antibody (Figure 4D). Immunohistochemistry showed much stronger staining of PITPNM3 in the cancer cell membrane and cytoplasm of all 192 cases of breast cancers on tissue arrays (Figure S4B) and 535 out of 562 cases on paraffin tissue sections (Table S1) than in the benign breast epithelia of 33 cases of fibrocystic disease (Figure 4E). PITPNM3 immunostaining in breast cancers was independent of $CCL18^+$ TAM counts ($p > 0.05$; Table S2). Interestingly, PITPNM3 expression was nearly absent in 83 cases of gastric cancers (Figure 4E; Figure S4B), implying that the two malignancies may respond distinctly to CCL18. This was further confirmed by western blot showing that PITPNM3 expression was much stronger in three breast cancer lines, including ER^+ MCF-7, $Her2^+$ BT-474, and triple-negative MDA-MB-231, than that in the immortalized MCF-10A breast epithelial line, but was barely detectable in two gastric cancer lines (Figure 4F).

To further confirm whether CCL18 colocalizes with PITPNM3 on breast cancer cell membrane, we incubated MDA-MB-231 cells with rCCL18 at 4°C for 3 hr. Confocal microscopy using fluorescence-labeled antibodies for CCL18 and PITPNM3 demonstrated that CCL18 colocalizes with PITPNM3 on the plasma membrane of MDA-MB-231 cells (Figure 4G). RNAi-mediated silencing of PITPNM3 expression in MDA-MB-231 cells (Figure S4C) efficiently abrogated CCL18 localization on the cell surface (Figure 4G), suggesting that CCL18 interacts with PITPNM3 at the plasma membrane of breast cancer cells.

Because PITPNM3 can be phosphorylated at its intracellular tyrosine residue (Lev et al., 1999), we investigated whether CCL18 might induce tyrosine phosphorylation of PITPNM3 by immunoprecipitating the membrane proteins extracted from rCCL18-treated MDA-MB-231 or MCF-10A cells with anti-PITPNM3. Immunoblot analysis of the immunoprecipitates using antibodies for phosphotyrosine and PITPNM3, respectively, demonstrated that rCCL18 dose dependently induced tyrosine phosphorylation of PITPNM3, whereas total PITPNM3 protein expression remained unchanged (Figures S4D and S4E).

To verify whether PITPNM3 is a functional receptor for CCL18, we created stable HEK293 lines expressing PITPNM3 (Figure S5A). Flow cytometry using an anti-PITPNM3 antibody demonstrated PITPNM3 localization at the cell surface of non-permeabilized stable PITPNM3 transfectants and MDA-MB-231 cells (Figure S5B). To provide a more refined assessment for PITPNM3 localization, we performed confocal microscopy for immunofluorescent staining of the protein in the stable transfectants and MDA-MB-231 cells that were costained with subcellular compartment trackers, and found that PITPNM3 primarily localized to the plasma membrane, but not to the endoplasmic reticulum or Golgi apparatus (Figure S5C). These results were further confirmed by western blot analysis of the PITPNM3 immunoprecipitates from the fractionated plasma and intracellular membranes (Figures S5D and S5E). We next measured the intracellular calcium ($[Ca^{2+}]_i$) changes upon CCL18 stimulation using calcium mobilization assay, which has been commonly used to measure chemokine receptor activation (Murdoch and Finn, 2000). PITPNM3 transfectants responded to rCCL18, but not to rCCL20, in a dose-dependant manner with an optimal concentration of 40 ng/ml, but transfectants with vector alone or nontransfected cells did not respond to the rCCL18 (Figure 5A; Figure S5F). Along with $[Ca^{2+}]_i$ changes, western blot analysis demonstrated that rCCL18 induced phosphorylation of PLCγ1 and PKCζ and increased the level of IP3KB, which are known mediators in the $[Ca^{2+}]$ signaling pathway (Figure 5B). To directly evaluate the ability of CCL18 to bind to PITPNM3, radioligand binding assays were performed. Because the parental 293 cells or cells transfected with vector alone did not bind to ^{125}I-CCL18 (data not shown), PITPNM3 transfectants showed a high level of specific binding for ^{125}I-CCL18, which could be competed by unlabeled CCL18 (K_d = 5.17 nM, 3.30–7.04 nM, 95% confidence interval; Figure 5C). Unlabeled CCL3 and CCL4 that show sequence homology to CCL18 by 64% and 48%, respectively (Schutyser et al., 2005), also competed for ^{125}I-CCL18 binding with much less affinity (K_d = 276.7 nM for CCL3, and K_d = 833 nM for CCL4), whereas CCL2 (35% homology) and CCL20 (28% homology) (Schutyser et al., 2005) had no apparent effect (Figure 5C). Specific binding of CCL18 to PITPNM3 on the surface of PITPNM3 transfectants could be further visualized by their costaining under confocal microscopy (Figure 5D). Next, we tested the ability of CCL18 to induce directional migration of PITPNM3 transfectants. As shown in Figure 5E, rCCL18, but not rCCL20, induced significant migration of PITPNM3 transfectants in a dose-dependent manner in vitro, whereas chemotaxis of the parental 293 cells and the cells transfected with vector alone was not affected by CCL18. In contrast, adding rCCL18 into the upper wells of the chemotaxis chambers at increasing concentrations dose dependently attenuated migration of the PITPNM3 transfectants in response to rCCL18 in the lower wells

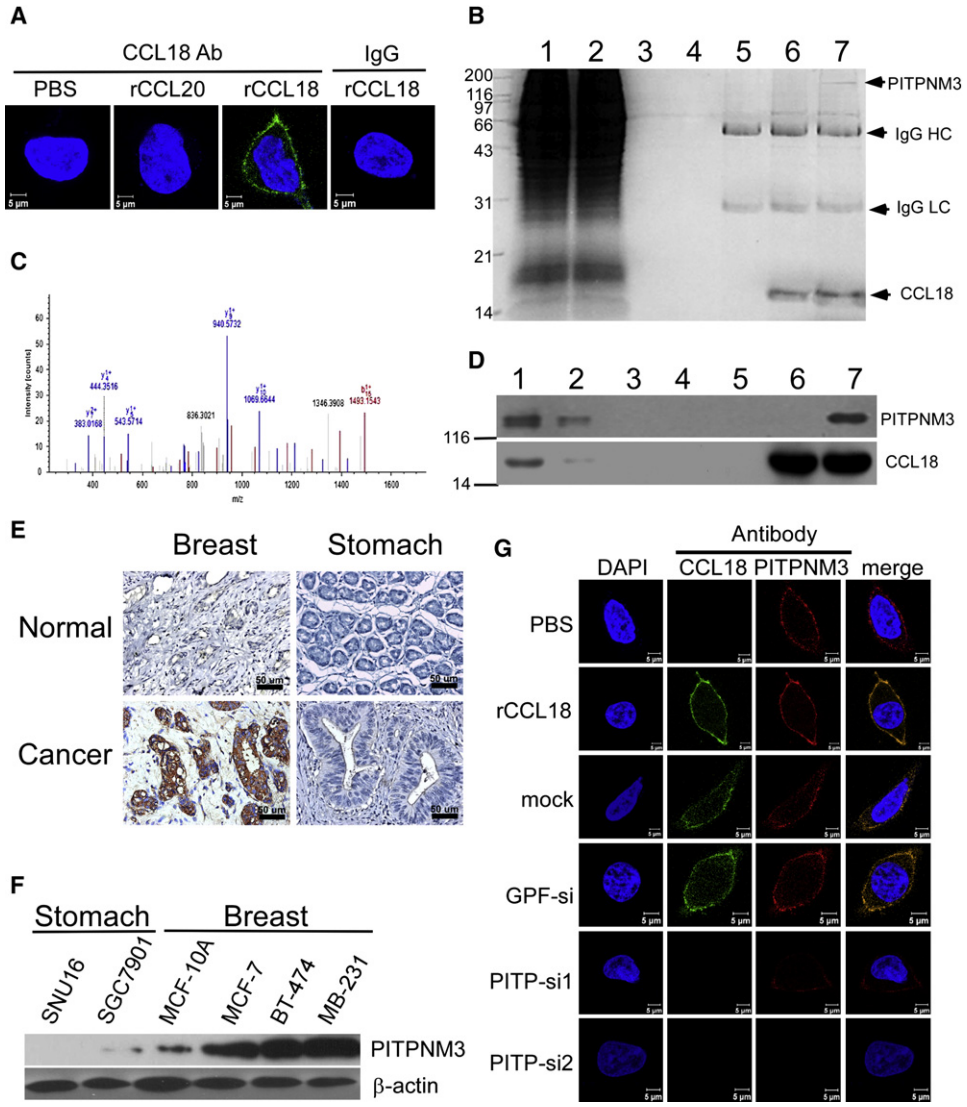

Figure 4. CCL18 Binds to PITPNM3 on Breast Cancer Cell Membrane

(A) Confocal microscopy for MDA-MB-231 cells treated with PBS, rCCL20, or rCCL18 at 20 ng/ml at 4°C, then fixed and stained with an Alexa 488-labeled anti-CCL18 antibody. An isotype-matched IgG (IgG) was used as a control, and cell nuclei were counterstained with DAPI.

(B) Immunoprecipitation of the membrane extracts (ME) from rCCL18-treated MDA-MB-231 cells with anti-CCL18 antibody. Lane 1 shows input of ME (5%), lane 2 flowthrough (5%), lane 3 ME from the PBS-treated cells incubated with uncoupled protein A/G beads, lane 4 ME from rCCL18-treated cells incubated with uncoupled beads, lane 5 ME from PBS-treated cells incubated with antibody-coupled beads, lane 6 SDS-treated ME from rCCL18-treated cells incubated with antibody-coupled beads, and lane 7 ME from rCCL18-treated cells incubated with antibody-coupled beads. IgG HC, IgG heavy chain; IgG LC, IgG light chain.

(C) Mass spectra of a representative peptide fragment from the protein band indicated by an arrow in lane 7 of (B).

(D) Western blot validation of mass spectrometric identification using an anti-PITPNM3 antibody (upper) and an anti-CCL18 antibody (lower). All lanes and conditions are described as in (B).

(E) Immunohistochemistry for PITPNM3 expression in breast and gastric carcinomas, as well as normal breast and gastric tissues in paraffin tissue sections.

(F) Western blotting for PITPNM3 expression in gastric cancer cell lines of SGC7901 and SNU16, breast epithelial MCF-10A line, and breast cancer cell lines of MCF-7, BT-474, and MDA-MB-231. β-Actin was used as a loading control.

(G) Confocal microscopy for MDA-MB-231 cells stained with an Alexa 488-labeled anti-CCL18 antibody and a Cy3-labeled anti-PITPNM3 antibody. The cells were treated with PBS (row 1) or recombinant CCL18 (rCCL18) at 20 ng/ml (rows 2–6) for 3 hr at 4°C, and were untransfected (row 2), mock transfected (row 3), transfected with GFP-siRNA (row 4), or either of the two PITPNM3-siRNAs (rows 5 and 6). Cell nuclei were counterstained with DAPI.

See also Figure S4.

(Figure 5F). Therefore, CCL18 specifically bound to PITPNM3, stimulated calcium signaling, and induced directional migration of the 293 cells with ectopic PITPNM3 expression, suggesting that PITPNM3 is a functional receptor for the chemokine.

PITPNM3 Mediates CCL18-Induced ECM Adherence and Invasion of Breast Cancer Cells

To further investigate the pathophysiological relevance of the CCL18-PITPNM3 interaction in breast cancer cells, we

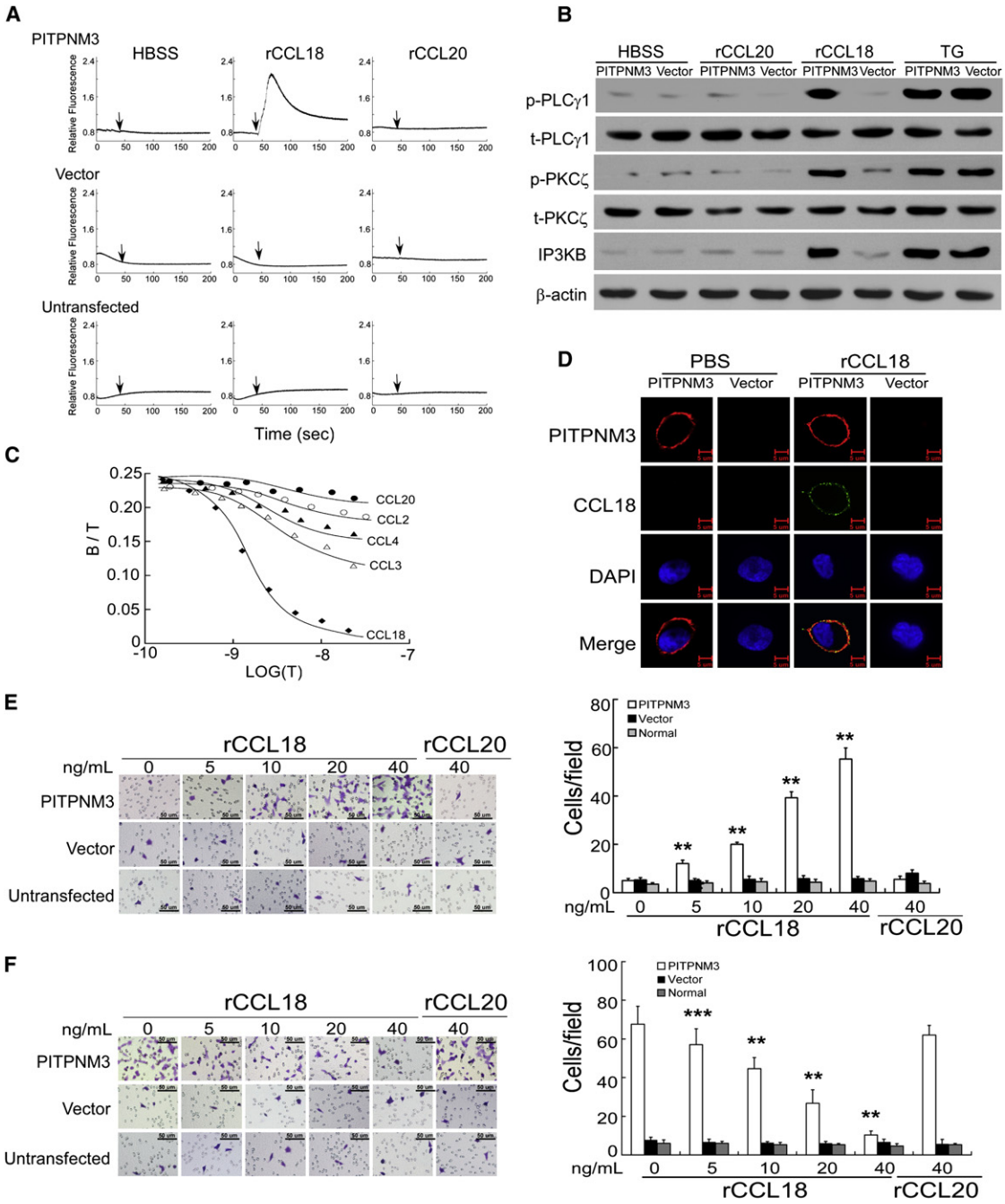

Figure 5. CCL18 Induces Functional Response in PITPNM3 Expressing HEK293 Cells

(A) Mobilization of $[Ca^{2+}]_i$ in HEK293 cells that were stably transfected with pcDNA3-PITPNM3 (PITPNM3), pcDNA3 vector alone (vector), or untransfected and were treated with HBSS, rCCL18, or rCCL20 at 40 ng/ml.

(B) Western blotting for the phosphorylated and total proteins of PLCγ1, PKCζ, and IP3KB in HEK293 cells that were transfected or treated as in (A). Thapsigargin (TG), a calcium channel agonist, was used as a positive control for calcium signaling.

(C) Binding assay with 60,000 cpm of ^{125}I-CCL18 in the presence or absence of increasing concentrations of unlabeled rCCL3, rCCL4, rCCL2, rCCL18, or rCCL20 for HEK293 cells that were transfected as in (A).

(D) Confocal microscopy for HEK293 cells stained with an Alexa 488-labeled anti-CCL18 antibody and a Cy3-labeled PITPNM3 antibody. The cells were transfected as in (A) and treated with PBS or rCCL18 at 40 ng/ml.

(E and F) Boyden chamber assays for HEK293 cells transfected as in (A) and treated with increasing concentrations of rCCL18 or rCCL20 at 40 ng/ml added to culture medium in the lower chambers (E), or added to culture medium in the upper chambers in the presence of rCCL18 at 20 ng/ml in the lower ones (F). Bars correspond to mean ± SD. **p < 0.01 and ***p < 0.001 as compared with the cells treated in the absence of rCCL18 in the lower (E) or the upper (F) chambers. See also Figure S5.

examined whether silencing of PITPNM3 influenced the biological effects of CCL18 on breast cancer cells. In the presence of rCCL18, transfection with either of the PITPNM3-siRNAs efficiently inhibited the adherence of MDA-MB-231 cells to fibronectin ($p < 0.001$; Figure 6A) and significantly reduced their invasiveness ($p < 0.001$; Figure 6B) to the level comparable to the cells without rCCL18 treatment ($p > 0.05$; Figures 6A and 6B). Transfection with PITPNM3-siRNA alone without rCCL18 treatment did not influence the adherence of MDA-MB-231 cells to fibronectin ($p > 0.05$; Figure 6A) or their invasiveness ($p > 0.05$; Figure 6B). These results suggest that the biological activities of CCL18 to promote invasiveness of breast cancer cells are PITPNM3 dependent.

Because PITPNM3 phosphorylation is associated with activation of proline-rich tyrosine kinase 2 (Pyk2) (Lev et al., 1999), one of the nonreceptor protein tyrosine kinases (NPTKs) at the focal adhesion complex (FAC), we examined whether CCL18 induced ECM adherence of the tumor cells via activating components of the FAC. Upon stimulation with rCCL18, phosphorylation of Pyk2 at Tyr402, Src at Tyr416, and FAK at Tyr397 was markedly induced in MDA-MB-231 cells, whereas the total protein levels remained unchanged (Figure 6C). However, transfection with PITPNM3-siRNA abrogated phosphorylation of the aforementioned NTPKs in MDA-MB-231 cells exposed to rCCL18 (Figure 6C), suggesting that CCL18 activates the NPTKs at the FAC of breast cancer cells by interacting with PITPNM3.

NPTK activation at the FAC may enhance ECM adherence of cancer cells via integrin clustering. Confocal microscopy of immunofluorescent staining with an anti-integrin $\alpha5\beta1$ antibody demonstrated prominent integrin clustering on the membrane of MDA-MB-231 cells treated with rCCL18 (Figure 6D). Abolition of FAK phosphorylation by RNAi-mediated silencing of PITPNM3 (Figure 6C) or FAK itself (Figure S6A) efficiently inhibited CCL18-induced integrin $\beta1$ clustering (Figure 6E) without altering the integrin expression (Figure S6A), which leads to tremendous reduction in fibronectin adherence of MDA-MB-231 cells (Figure 6F). Additionally, silencing integrin $\beta1$ (Figure S6B) in the presence of CCL18 prevented their own clustering (Figure 6E) and fibronectin adherence of the tumor cells (Figure 6F) but did not affect total FAK expression or FAK phosphorylation (Figure S6B), suggesting that FAK activation induced by CCL18-PITPNM3 interaction is independent of integrin $\beta1$ signaling. More importantly, abrogation of integrin clustering or fibronectin adherence by FAK-siRNA or integrin-$\beta1$-siRNA significantly reduced the invasion of MDA-MB-231 cells in Boyden chambers (Figure 6G). Collectively, these data suggest that integrin clustering and fibronectin adherence mediated by FAK activation due to CCL18-PITPNM3 interaction contribute to the overall process of CCL18-induced invasion in the breast cancer cells.

CCL18 Enhances Invasion and Metastasis of Breast Cancers In Vivo

To examine the effect of CCL18-PITPNM3 interaction on breast cancer invasion and metastasis in vivo, we inoculated BT-474 cells (low metastasis potential) and MDA-MB-231 cells (high metastasis potential) into the mammary fat pads of NOD/SCID mice, and evaluated cancer metastasis to the lungs and livers when xenografts reached 1.5 cm in diameter. Intratumor injection of rCCL18 at a dosage of 0.1 μg/kg biweekly for 4 consecutive weeks, but not PBS or rCCL20 at the same dosage, enhanced vascular invasion and penetration of BT-474 cancer cells into adjacent normal tissues (Figure 7A).

Although injection of rCCL18 into BT-474 and MDA-MB-231 xenografts did not obviously change the primary tumor size (Figure S7A), it increased the number of mice with lung and liver metastases (Table S4), the average lung weight (Figure 7B), and the number of metastatic nodules in the livers (Figures S7B and S7C). When the mice were xenografted with BT-474 and MDA-MB-231 cells that stably express luciferase, luminescence imaging for the harvested lungs and livers demonstrated that the severity of lung and liver metastasis was promoted by treatment with rCCL18 (Figure 7C). Hematoxylin and eosin staining (H&E) also showed that rCCL18 injection led to more massive metastasis in the lungs and livers of the mice bearing BT-474 or MDA-MB-231 xenografts as compared with PBS or rCCL20 injection (Figures 7D and 7F). Quantification of human HPRT mRNA also demonstrated that rCCL18 increased the number of metastatic breast cancer cells in both lungs and livers by 5.5- and 3.2-fold, respectively, in the BT-474 xenografted mice, and by 2.7- and 2.6-fold, respectively, in the MDA-MB-231 xenografted mice as compared with PBS injection (Figures 7E and 7G). More importantly, Kaplan-Meier analysis demonstrated that rCCL18 injection reduced the survival of the mice xenografted with BT-474 or MDA-MB-231 cells compared with PBS or rCCL20 injection (Figure 7H). Collectively, these data suggest that CCL18 enhances lung and liver metastases of breast cancer xenografts.

Furthermore, rCCL18 failed to enhance the vascular invasion and peritumoral penetration of BT-474 xenografts infected with lenti-PITPNM3-shRNA, but not with lenti-GFP-shRNA (Figure 7A). Silencing PITPNM3 also alleviated the promoting effect of rCCL18 on lung and liver metastases of BT-474 and MDA-MB-231 xenografts (Table S4; Figures 7 B–7G) and abrogated CCL18-induced reduction in mouse survival and body weight (Figures 7H and 7I). These results suggest that CCL18 promotes invasion and metastasis of breast cancers in vivo in a PITPNM3-dependent manner.

To further evaluate whether CCL18 promotes in vivo metastasis by enhancing ECM adherence via FAK activation and integrin clustering, we performed intratumor injection of synthetic FAK-siRNA or integrin-$\beta1$-siRNA in BT474 xenografts 48 hr prior to each episode of rCCL18 administration. Although injection of FAK-siRNA or integrin-$\beta1$-siRNA did not obviously alter primary tumor size (Figure S7D), transient silencing of FAK or integrin-$\beta1$ significantly alleviated CCL18-promoting metastasis to the lungs and the livers (Figures S7E–S7I), and prolonged mouse survival upon CCL18 treatment (Figure S7J). Similar results were obtained in the NOD/SCID mice xenografted with MDA-MB-231 cells (data not shown). Therefore, CCL18-induced ECM adherence of breast cancer cells ultimately contributes to in vivo metastasis.

DISCUSSION

TAM-featured inflammation is known as the seventh hallmark of cancer'' (Condeelis and Pollard, 2006; Pollard, 2004). Although M1 macrophage is linked with tumoricidal activity, M2 macrophage is associated with cancer progression and metastasis

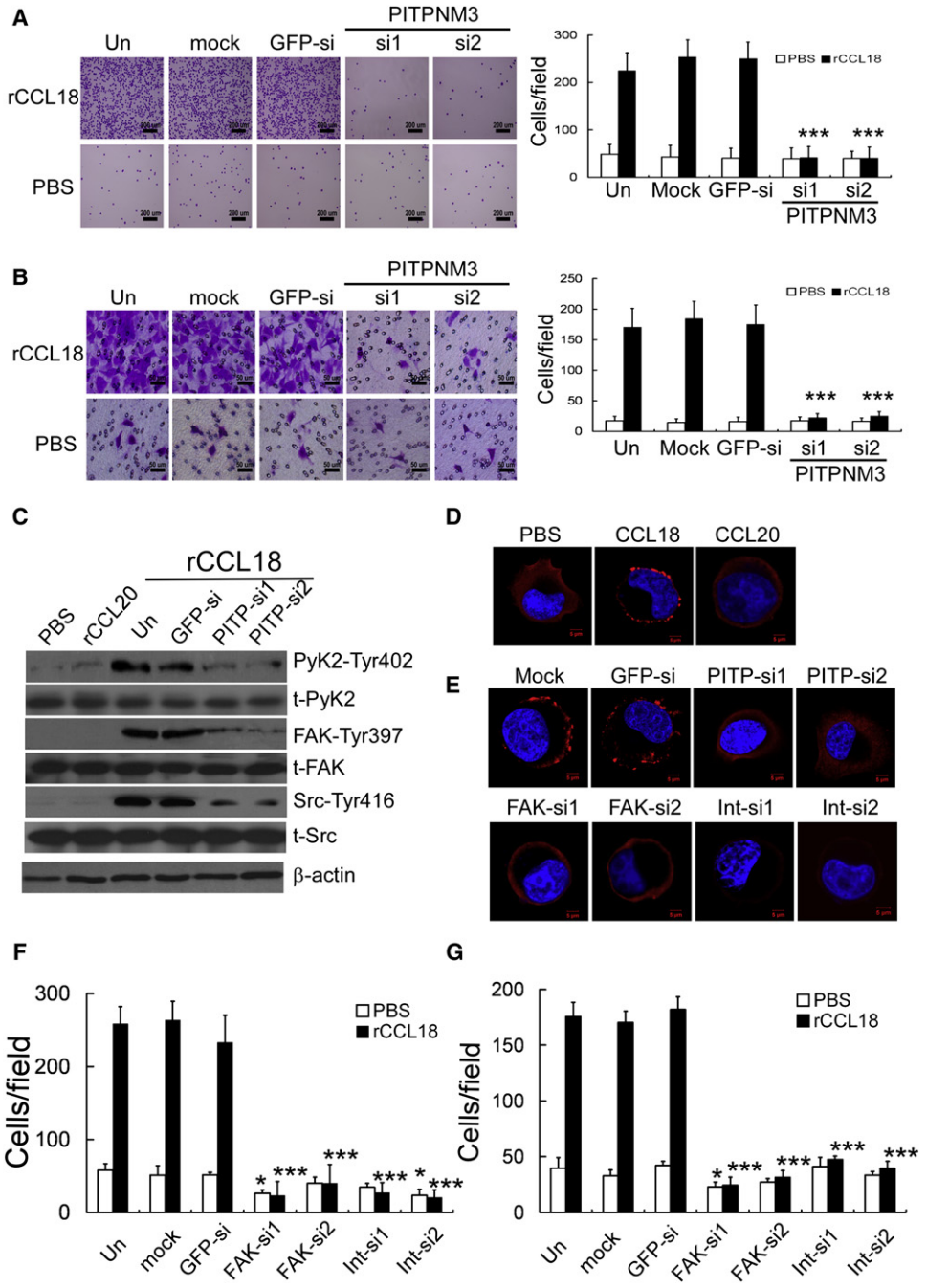

Figure 6. CCL18 Enhances Fibronectin Adherence and Invasiveness of Breast Epithelial Cells via Interacting with PITPNM3

(A) Adherence assay for MDA-MB-231 cells that were mock transfected, or transfected with GFP-siRNA or either of the PITPNM3-siRNAs, and were treated with PBS or rCCL18 at 20 ng/ml.

(B) Boyden chamber assay for the MDA-MB-231 cells that were treated as in (A). Bars correspond to mean ± SD. ***$p < 0.001$ versus untransfected control (Un).

(C) Western blotting of MDA-MB-231 cells treated with PBS, rCCL20, or rCCL18 with or without transfection of GFP-siRNA or either of the PITPNM3-siRNAs for the expression of the phosphorylated and total proteins of Pyk2, FAK, and Src; β-actin was used as a loading control.

(D and E) Confocal microscopy of integrin α5β1 staining of PBS-treated or rCCL18-treated MDA-MB-231 cells that were untransfected (D), or mock transfected, transfected with PITPNM3-siRNAs, FAK-siRNAs, integrin-β1-siRNAs, or GFP-siRNA (E).

(F) Adherence assays for MDA-MB-231 cells that were untransfected, mock transfected, or transfected with GFP-siRNA or either of the FAK-siRNAs or integrin-β1-siRNAs in the presence or absence of rCCL18 at 20 ng/ml.

(G) Boyden chamber assay for MDA-MB-231 cells that were untransfected (Un), mock transfected, or transfected with FAK-siRNAs, integrin-β1-siRNAs, or GFP-siRNA, followed by treatment for 8 hr with PBS or rCCL18. Bars correspond to mean ± SD. *$p < 0.05$ and ***$p < 0.001$ as compared with the untransfected cells.

See also Figure S6.

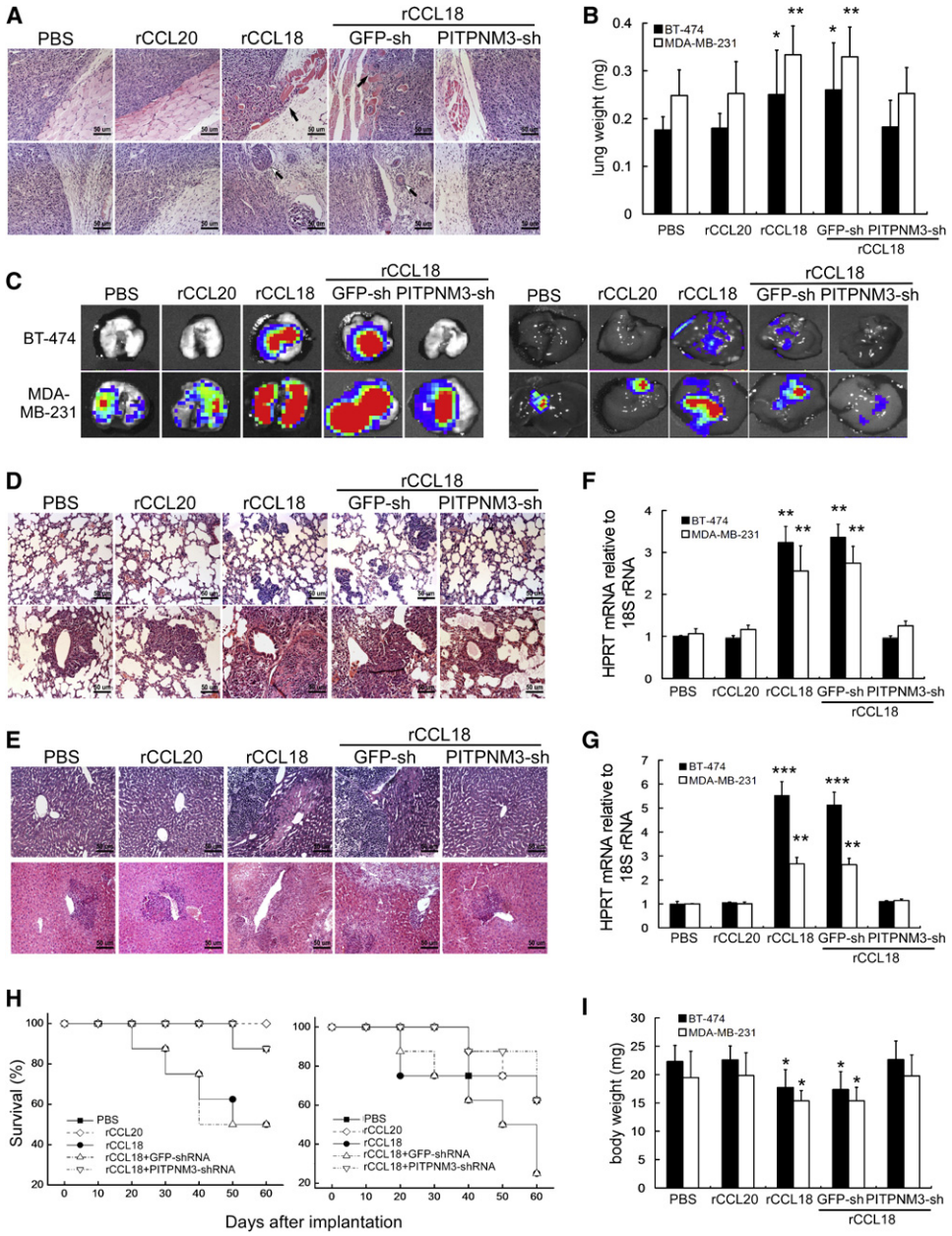

Figure 7. CCL18 Promotes Lung and Liver Metastasis of Breast Cancer Xenografts via PITPNM3

(A) Microscopic images of H&E for breast cancer xenografts demonstrating the presence or absence of margin invasion (upper) and vascular invasion (lower) of BT-474 tumors.

(B) Wet lung weight in tumor-bearing mice. Bars correspond to mean ± SD.

(C) Luminal images of the lungs (left) and livers (right) of tumor-bearing mice.

(D and F) H&E of the lungs (D) and livers (F) in the mice-bearing BT-474 (upper) and MDA-MB-231 (lower) xenografts.

(E and G) Expression of human HPRT mRNA relative to mouse 18S rRNA in the lungs (E) and livers (G) of the tumor-bearing mice. Data are normalized to PBS-treated mice.

(H) Kaplan-Meier survival curve for the mice-bearing BT-474 (left) and MDA-MB-231 xenografts (right).

(I) Body weight of tumor-bearing mice. Bars correspond to mean ± SD. *$p < 0.05$, **$p < 0.01$, and ***$p < 0.001$ as compared with PBS-treated mice.

See also Figure S7,and Tables S4 and S5.

(Mancino and Lawrence, 2010). It was recently reported that breast TAMs are primarily a polarized M2 macrophage population (DeNardo et al., 2009). Here, we showed that CCL18, a characteristic C-C chemokine released by M2 macrophages, is abundantly expressed in breast TAMs and correlates with the metastasis and poor prognosis of patients with breast cancer.

Chemokines exert their effects by binding to specific transmembrane receptors, which are members of a large family

of G protein-coupled receptors (GPCRs). Currently, 22 chemokine receptors have been characterized to mediate the effects of more than 47 known chemokines, with overlapping specificities for one another (Jin et al., 2008). Recent studies have demonstrated that tumor cells also express restricted and specific patterns of chemoreceptors (Lazennec and Richmond, 2010; Vandercappellen et al., 2008). Although CCL18-induced chemotaxis in naive T cells was suggested to be mediated by GPCR (Adema et al., 1997), the cognate receptor and downstream-signaling pathways of CCL18 remained unknown. Our data reveal that CCL18 specifically binds to PITPNM3 at the cellular membrane of breast cancer cells to exert its biological activities. Several lines of our evidence in HEK293 cells stably transfected with PITPNM3 support the conclusion that PITPNM3 is a functional receptor for CCL18. These were obtained from functional assays that had traditionally been used to characterize chemokine receptors (Murdoch and Finn, 2000), including high-affinity binding of CCL18 to PITPNM3, dose-dependent mobilization of $[Ca^{2+}]_i$, activation of the mediators in the $[Ca^{2+}]$ signaling pathway, and directional migration of PITPNM3 transfectants in response to CCL18. Furthermore, our data demonstrated that PITPNM3 served as an essential CCL18 receptor in breast cancer cells to mediate CCL18 effects of promoting invasion and metastasis.

PITPNM3, also named Nir1, was shown to be expressed in human retina, brain, spleen, and ovary (Lev et al., 1999). Our study demonstrated that PITPNM3 is abundantly expressed in breast cancer cells. In contrast to other members in the family of the PYK2-binding proteins, such as Nir2 and Nir3 that are associated with endoplasmic reticula and Golgi complex (Lev, 2004; Amarilio et al., 2005), PITPNM3/Nir1 is localized at the plasma membrane of breast cancer cells and HEK293 transfectants. PITPNM3 expression is essential to CCL18-induced calcium influx and chemotaxis, which could be completely abrogated by pretreatment with a GPCR pathway inhibitor, pertussis toxin (PTX) (data not shown). These results suggest that PITPNM3 is a GPCR. However, previously identified chemokine receptors are seven-transmembrane GPCRs, and PITPNM3 was suggested as a putative six-transmembrane protein because its primary structures harbor six hydrophobic stretches (Lev et al., 1999). Nevertheless, it has been reported that truncated version of five-transmembrane proteins is sufficient to exert GPCR function (Ling et al., 1999). In light of the large structural diversity and lack of consensus motif at the intracellular regions of GPCRs (Wong, 2003), conformation at the intracellular region of PITPNM3 may determine G protein selection and activation for downstream intracellular signaling events, which needs further study.

Our findings of extensive PITPNM3 expression and its functional role in breast cancer cells support the correlation of CCL18-expressing TAM count and patient prognosis because more CCL18 produced by TAMs may exert a stronger metastasis-promoting effect on breast cancer cells expressing PITPNM3. In contrast, PITPNM3 is barely detected in gastric cancer cells, and $CCL18^+$ TAMs are positively associated with patient survival in gastric cancer (Leung et al., 2004). The disparity of PITPNM3 expression between breast and gastric cancers may suggest that gastric cancer cells do not respond to CCL18 in the same way as breast cancer cells, which may explain the distinct clinical outcomes of the two malignancies associated with $CCL18^+$ TAM counts.

It has been shown that ECM adherence of tumor cells is a key biological process for epithelial tumor cells to increase invasiveness (Thiery et al., 2009). CCL18 triggers integrin clustering and ECM adherence of the tumor cells, which eventually contribute to enhanced invasiveness and metastasis. The molecular mechanism responsible for these phenomena is activating phosphorylation of FAK in the FAC mediated by PITPNM3, which is independent of integrin expression. It has been noted that Pyk2, a key component of the FAC, interacts with PITPNM3 (Lev et al., 1999), and Pyk2 is associated with other NRTKs at the FAC, such as Src and FAK, which may form the basis of FAK activation and ECM adherence when PITPNM3 is ligated with CCL18. In the stroma of invasive carcinomas, TAMs produce a variety of proteases, including uPA and various matrix metalloproteinases, to degrade the basement membrane and the surrounding ECM, leading to the exposure of the fibronectin molecules to tumor cells (Pollard, 2004). By enhancing the adhesion of the dissociated breast cancer cells to the exposed fibronectin, CCL18 may assist cancer cells to penetrate and migrate through the tumor stroma and ultimately egress into lymphatic or blood vessels for regional or distal metastasis (Thiery et al., 2009).

In summary our study shows that PITPNM3 is a functional receptor for CCL18, an important TAM-derived cytokine, in promoting breast cancer metastasis. Other TAM-derived chemokines or growth factors (Coussens et al., 2000; Dirkx et al., 2006; Goswami et al., 2005; Leek et al., 2002) may also contribute via other signaling pathways because suppression of CCL18 or PITPNM3 did not completely block breast cancer metastasis elicited by TAMs. Further studies are needed to evaluate whether the cytokine repertoire released by TAMs can be manipulated to inhibit tumor progression.

EXPERIMENTAL PROCEDURES

Patients and Tissue Samples

Primary ductal carcinomas of the breasts were obtained from 562 female patients (median age 48.5 years, range 21–79) at the No. 2 Affiliated Hospital, Sun-Yat-Sen University, from January 2002 to October 2007. Pathological diagnosis, as well as ER and Her2 status, was verified by two different pathologists. Patients with invasive carcinomas, other than DCIS, underwent six cycles of postoperative adjuvant chemotherapy with FAC regimen (5-fluorouracil 500 mg/m^2, doxorubicin 50 mg/m^2, and cyclophosphamide 500 mg/m^2). Subsequently, patients with ER^+ tumors underwent endocrine therapy according to NCCN guideline. Distal metastasis was not found in these patients upon diagnosis but was identified in 105 cases during postoperative follow-up. Additionally, benign breast tissue samples were collected from 61 cases of cystic fibrosis of the breast with or without atypical epithelial hyperplasia. All samples were collected with informed consent according to the Internal Review and the Ethics Boards of the Sun-Yat-Sen Memorial Hospital of Sun-Yat-Sen University.

Cell Cultures and Treatment

MDA-MB-231, MDA-MB-435s, BT-474, SKBR3, and MCF-7 breast cancer cells, MCF-10A breast epithelial cells, SNU16 and SGC7901 gastric cancer cells, and HEK293 embryonic kidney cells were obtained from American Type Culture Collection (ATCC) and grown according to standard protocols. PBMs from patients with breast cancer or healthy donors were isolated by density-gradient centrifugation using Ficoll-Hypaque (Pharmacia). Primary breast cancer cells were isolated from eight cases of freshly removed tumor

samples using Cell Isolation Kit (Panomics) according to the manufacturer's instruction, and TAMs were isolated from 47 fresh tumor samples with a Percoll Density Gradient Centrifugation kit (Pharmacia).

Affinity Purification of CCL18-Interacting Proteins

MDA-MB-231 cells were grown to 75% confluence followed by treatment for 60 min with 20 ng/ml rCCL18 in serum-free medium. Membrane proteins of the treated cells were extracted using a ProteoExtract Native Membrane Protein Extraction Kit (M-PEK Kit; Calbiochem) according to manufacturer's instruction. As a control, 0.1% sodium dodecyl sulfate (SDS) was added into the solubilized extracts to disrupt the interaction between rCCL18 and the unknown receptor, and SDS was then removed by precipitation using an SDS-Out Precipitation Kit (Pierce). The solubilized extracts were then incubated with 30 μl of protein A/G beads coupled to a mouse anti-human monoclonal CCL18 antibody (R&D) at room temperature for 2 hr. The beads were then washed with lysis buffer three times, followed by boiling in 1× sample buffer. The immunoprecipitates were resolved on an SDS-PAGE denaturing gel, visualized by Coomassie blue, and the protein band of interest was removed for mass spectrometric analysis.

Tumor Xenografts

Female NOD/LtSz-scid/scid (NOD/SCID) mice were bred and maintained under defined conditions at the Animal Experiment Center of Sun-Yat-Sen University, and all procedures were approved by the Animal Care and Use Committee of Sun-Yat-Sen University and conformed to the legal mandates and national guidelines for the care and maintenance of laboratory animals. Breast cancer MDA-MB-231-luc (2×10^6) and BT-474 cells-luc (5×10^6) that were uninfected or infected with lentivirus carrying GFP-shRNA or PITPNM3-shRNA were inoculated into the mammary fat pads of the mice (n = 8/group). When the xenografts were palpable (around 0.5 cm in diameter), intratumor injection of PBS, rCCL20, or rCCL18 at 0.1 μg/kg was performed biweekly for 4 consecutive weeks. In some experiments, intratumor injection of PBS, lipofectamine (5 μl) alone or in complex with integrin-β1-siRNA, FAK-siRNA, or GFP-siRNA at 2 mg/kg was performed 48 hr prior to CCL18 injection. Tumor growth was evaluated by monitoring tumor volume (TV = length × width^2 × 0.5) every 3 days for 8 weeks. The animals were sacrificed when the xenografts reached 1.5 cm in diameter, and tumor xenografts, lungs, and livers of the mice were harvested for further evaluation. Cryosections (4 μm) of the harvested organs were H&E for histological assessment, and total RNA was extracted for qRT-PCR analysis of human HPRT mRNA expression. The lungs and livers of the animals bearing breast tumor xenografts that stably express luciferase were analyzed by IVIS Lumina Imaging System (Xenogen).

Statistics

All statistical analyses were done using SPSS for Windows version 13.0 (SPSS, Chicago). Student's t test and one-way ANOVA were used to correlate serum CCL18 level with cancer metastasis, whereas chi-square test was applied to analyze the relationship between CCL18+ TAM counts and clinicopathological status. Kaplan-Meier survival curves were plotted, and log rank test was done. The significance of various variables for survival was analyzed by the Cox proportional hazards model in a multivariate analysis. All experiments for cell cultures were performed independently for at least five times and in triplicate for each time. A p value <0.05 in all cases was considered statistically significant.

SUPPLEMENTAL INFORMATION

Supplemental Information includes Seven Figures, Four Tables, and Supplemental Experimental Procedures and can be found with this article online at doi:10.1016/j.ccr.2011.02.006.

ACKNOWLEDGMENTS

This work was supported by grants from 973 (2010CB912800, 2011CB504203, 2009CB521706,2008ZX10208, 2010CB912103) Projects from Ministry of Science and Technology of China, the Natural Science Foundation of China (30921140312,30831160515, 30830110, 30772550, 30671930, 30972785, 30973396, 30973505, 30801376, 90913016, 30900497), Chinese Academy of Science (KSCX1-YW-R65, KSCX2-YW-H-10, and KSCX2-YW-R-195), and Natural Science Foundation of Guangdong Province (8251008901000011), Key Laboratory of malignant tumor gene regulation and target therapy of Guangdong Higher Education Institutes, Sun Yat-sen University (KLB09001). A Key Project from Anhui Province (08040102005).

Received: June 16, 2010
Revised: November 8, 2010
Accepted: February 3, 2011
Published: April 11, 2011

REFERENCES

Adema, G.J., Hartgers, F., Verstraten, R., de Vries, E., Marland, G., Menon, S., Foster, J., Xu, Y., Nooyen, P., McClanahan, T., et al. (1997). A dendritic-cell-derived C-C chemokine that preferentially attracts naive T cells. Nature *387*, 713–717.

Amarilio, R., Ramachandran, S., Sabanay, H., and Lev, S. (2005). Differential regulation of endoplasmic reticulum structure through VAP-Nir protein interaction. J. Biol. Chem. *280*, 5934–5944.

Chang, C.Y., Lee, Y.H., Leu, S.J., Wang, C.Y., Wei, C.P., Hung, K.S., Pai, M.H., Tsai, M.D., and Wu, C.H. (2010). CC-chemokine ligand 18/pulmonary activation-regulated chemokine expression in the CNS with special reference to traumatic brain injuries and neoplastic disorders. Neuroscience *165*, 1233–1243.

Condeelis, J., and Pollard, J.W. (2006). Macrophages: obligate partners for tumor cell migration, invasion, and metastasis. Cell *124*, 263–266.

Coussens, L.M., Tinkle, C.L., Hanahan, D., and Werb, Z. (2000). MMP-9 supplied by bone marrow-derived cells contributes to skin carcinogenesis. Cell *103*, 481–490.

DeNardo, D.G., Barreto, J.B., Andreu, P., Vasquez, L., Tawfik, D., Kolhatkar, N., and Coussens, L.M. (2009). CD4(+) T cells regulate pulmonary metastasis of mammary carcinomas by enhancing protumor properties of macrophages. Cancer Cell *16*, 91–102.

Dirkx, A.E., Oude Egbrink, M.G., Wagstaff, J., and Griffioen, A.W. (2006). Monocyte/macrophage infiltration in tumors: modulators of angiogenesis. J. Leukoc. Biol. *80*, 1183–1196.

Duluc, D., Corvaisier, M., Blanchard, S., Catala, L., Descamps, P., Gamelin, E., Ponsoda, S., Delneste, Y., Hebbar, M., and Jeannin, P. (2009). Interferon-gamma reverses the immunosuppressive and protumoral properties and prevents the generation of human tumor-associated macrophages. Int. J. Cancer *125*, 367–373.

Gocheva, V., Wang, H.W., Gadea, B.B., Shree, T., Hunter, K.E., Garfall, A.L., Berman, T., and Joyce, J.A. (2010). IL-4 induces cathepsin protease activity in tumor-associated macrophages to promote cancer growth and invasion. Genes Dev. *24*, 241–255.

Gordon, S. (2003). Alternative activation of macrophages. Nat. Rev. Immunol. *3*, 23–35.

Goswami, S., Sahai, E., Wyckoff, J.B., Cammer, M., Cox, D., Pixley, F.J., Stanley, E.R., Segall, J.E., and Condeelis, J.S. (2005). Macrophages promote the invasion of breast carcinoma cells via a colony-stimulating factor-1/epidermal growth factor paracrine loop. Cancer Res. *65*, 5278–5283.

Jin, T., Xu, X., and Hereld, D. (2008). Chemotaxis, chemokine receptors and human disease. Cytokine *44*, 1–8.

Kodelja, V., Muller, C., Politz, O., Hakij, N., Orfanos, C.E., and Goerdt, S. (1998). Alternative macrophage activation-associated CC-chemokine-1, a novel structural homologue of macrophage inflammatory protein-1 alpha with a Th2-associated expression pattern. J. Immunol. *160*, 1411–1418.

Lazennec, G., and Richmond, A. (2010). Chemokines and chemokine receptors: new insights into cancer-related inflammation. Trends Mol. Med. *16*, 133–144.

Leek, R.D., Talks, K.L., Pezzella, F., Turley, H., Campo, L., Brown, N.S., Bicknell, R., Taylor, M., Gatter, K.C., and Harris, A.L. (2002). Relation of hypoxia-inducible factor-2 alpha (HIF-2 alpha) expression in tumor-infiltrative

macrophages to tumor angiogenesis and the oxidative thymidine phosphorylase pathway in Human breast cancer. Cancer Res. *62*, 1326–1329.

Leung, S.Y., Yuen, S.T., Chu, K.M., Mathy, J.A., Li, R., Chan, A.S., Law, S., Wong, J., Chen, X., and So, S. (2004). Expression profiling identifies chemokine (C-C motif) ligand 18 as an independent prognostic indicator in gastric cancer. Gastroenterology *127*, 457–469.

Lev, S. (2004). The role of the Nir/rdgB protein family in membrane trafficking and cytoskeleton remodeling. Exp. Cell Res. *297*, 1–10.

Lev, S., Hernandez, J., Martinez, R., Chen, A., Plowman, G., and Schlessinger, J. (1999). Identification of a novel family of targets of PYK2 related to Drosophila retinal degeneration B (rdgB) protein. Mol. Cell. Biol. *19*, 2278–2288.

Lichtenberger, B.M., Tan, P.K., Niederleithner, H., Ferrara, N., Petzelbauer, P., and Sibilia, M. (2010). Autocrine VEGF signaling synergizes with EGFR in tumor cells to promote epithelial cancer development. Cell *140*, 268–279.

Ling, K., Wang, P., Zhao, J., Wu, Y.L., Cheng, Z.J., Wu, G.X., Hu, W., Ma, L., and Pei, G. (1999). Five-transmembrane domains appear sufficient for a G protein-coupled receptor: functional five-transmembrane domain chemokine receptors. Proc. Natl. Acad. Sci. USA *96*, 7922–7927.

Mancino, A., and Lawrence, T. (2010). Nuclear factor-kappaB and tumor-associated macrophages. Clin. Cancer Res. *16*, 784–789.

Mantovani, A., and Sica, A. (2010). Macrophages, innate immunity and cancer: balance, tolerance, and diversity. Curr. Opin. Immunol. *22*, 231–237.

Mantovani, A., Marchesi, F., Porta, C., Sica, A., and Allavena, P. (2007). Inflammation and cancer: breast cancer as a prototype. Breast *16* (*Suppl 2*), S27–S33.

Martinez, F.O., Helming, L., and Gordon, S. (2009). Alternative activation of macrophages: an immunologic functional perspective. Annu. Rev. Immunol. *27*, 451–483.

Murdoch, C., and Finn, A. (2000). Chemokine receptors and their role in inflammation and infectious diseases. Blood *95*, 3032–3043.

Pittet, M.J. (2009). Behavior of immune players in the tumor microenvironment. Curr. Opin. Oncol. *21*, 53–59.

Pollard, J.W. (2004). Tumour-educated macrophages promote tumour progression and metastasis. Nat. Rev. Cancer *4*, 71–78.

Robinson, B.D., Sica, G.L., Liu, Y.F., Rohan, T.E., Gertler, F.B., Condeelis, J.S., and Jones, J.G. (2009). Tumor microenvironment of metastasis in human breast carcinoma: a potential prognostic marker linked to hematogenous dissemination. Clin. Cancer Res. *15*, 2433–2441.

Schutyser, E., Richmond, A., and Van Damme, J. (2005). Involvement of CC chemokine ligand 18 (CCL18) in normal and pathological processes. J. Leukoc. Biol. *78*, 14–26.

Schutyser, E., Struyf, S., Proost, P., Opdenakker, G., Laureys, G., Verhasselt, B., Peperstraete, L., Van de Putte, I., Saccani, A., Allavena, P., et al. (2002). Identification of biologically active chemokine isoforms from ascitic fluid and elevated levels of CCL18/pulmonary and activation-regulated chemokine in ovarian carcinoma. J. Biol. Chem. *277*, 24584–24593.

Simpson-Haidaris, P.J., and Rybarczyk, B. (2001). Tumors and fibrinogen. The role of fibrinogen as an extracellular matrix protein. Ann. N Y Acad. Sci. *936*, 406–425.

Solinas, G., Germano, G., Mantovani, A., and Allavena, P. (2009). Tumor-associated macrophages (TAM) as major players of the cancer-related inflammation. J. Leukoc. Biol. *86*, 1065–1073.

Thiery, J.P., Acloque, H., Huang, R.Y., and Nieto, M.A. (2009). Epithelial-mesenchymal transitions in development and disease. Cell *139*, 871–890.

Vandercappellen, J., Van Damme, J., and Struyf, S. (2008). The role of CXC chemokines and their receptors in cancer. Cancer Lett. *267*, 226–244.

Wong, S.K. (2003). G protein selectivity is regulated by multiple intracellular regions of GPCRs. Neurosignals *12*, 1–12.

Zohny, S.F., and Fayed, S.T. (2010). Clinical utility of circulating matrix metalloproteinase-7 (MMP-7), CC chemokine ligand 18 (CCL18) and CC chemokine ligand 11 (CCL11) as markers for diagnosis of epithelial ovarian cancer. Med. Oncol. *27*, 1246–1253.